circRNA-miRNA-mRNA networks reveal a proangiogenic action of circNPHP1 in human ischemic heart disease

[1]Maryam Anwar*, [1]Moumita Sarkar*, [2]Kerrie Ford, [2]Gianni D Angelini,
[1,3]Prakash Punjabi, [1]Abas Laftah,[1]Aránzazu Chamorro-Jorganes,
[1]Jiahui Ji, [1]Prashant K Srivastava, [4]Enrico Petretto; [1]Costanza Emanueli

[1] National Heart and Lung Institute, Imperial College London, London, UK
[2]Bristol Heart Institute, University of Bristol, UK
[3] NHS trust, Imperial College London, London, UK
[4]Centre for Computational Biology, Duke-NUS Medical School, Singapore

*Similar contribution

Address for correspondence:
Dr. Maryam Anwar
Imperial College London
72 Du Cane Road, London W12 0NN
e-mail: maryam.anwar@imperial.ac.uk

Prof. Costanza Emanueli
Imperial College London
72 Du Cane Road, London W12 0NN
e-mail: e.emanueli@imperial.ac.uk

ABSTRACT

Background: Ischemic heart disease (IHD) is characterized by insufficient myocardial blood flow and aggravated by diabetes. IHD is often treated by coronary revascularization. Complementary therapies that increase the microvascular flow by promoting endothelial homeostasis and repair are still lacking and require the identification of new therapeutic targets. The expression of protein coding genes is regulated by multimodal interactions between different classes of non-coding RNAs. This study aimed to 1) unravel circular RNA (circRNA) -microRNA (miRNA) - messenger RNA (mRNA) networks across the human ischemic and control hearts; 2) identify and functionally test the sub-network with highest potential to control endothelial cell (EC) function.

Methods: Two intraoperative left ventricle biopsies were prospectively collected from type-2 diabetic and non-diabetic people with IHD and from a control group of non-IHD, non-diabetic patients (N=12 patients/group; ARCADIA study) and used for long transcriptome bulk-sequencing (circRNAs and mRNAs datasets) and small RNA-sequencing (miRNAs datasets). Differentially expressed (DE) RNAs were identified with a customized bioinformatics pipeline. We identified potential "sponging associations" between circRNAs and miRNAs and between miRNAs and mRNAs. Next, we created circRNA-miRNA-mRNA networks and retained the subnetworks where individual RNAs were expressed in ECs (using datasets from GEO database) and of potential relevance to endothelial function based on pathway analyses. Next, we screened top differentially expressed circRNAs in cultured ECs exposed to disease-mimic conditions vs control. The circRNA-miRNA sponging interactions of the top emerging circRNA candidate were confirmed after circRNA pulldown in ECs and the functional relevance was mechanistically tested in EC cell biology assays.

Results: We created circRNA-miRNA-mRNA networks in IHD (with and without T2DM) and controls indicating distinct interactions in each. We unravelled a novel putative proangiogenic subnetwork, circNPHP1/miR-221-3p/VEGFA/BCL2, in the human ischemic heart specially enriched in IHD and T2DM. CircNPHP1 pull-down assay confirmed it's binding to miR-221-3p. CircNPHP1 silencing in ECs reduced angiogenesis and decreased the expression of miR-221-3p target genes (VEGFA and BCL2). The proangiogenic action of circNPHP1/miR-221-3p was confirmed in ECs by

combining circNPHP1 silencing with either miR-221-3p inhibition or overexpression in ECs.

Conclusions: CircNPHP1 supports endothelial function through sponging of miR-221-3p in IHD and holds potential as novel therapeutic target in IHD.

Keywords: Ischemic heart disease; cardiovascular disease; angiogenesis; circRNA; miRNA; RNA networks.

INTRODUCTION

Severe coronary atherosclerosis promotes ischemic heart disease (IHD). This pathogenic process is aggravated by Type 2 diabetes mellitus (T2DM). Ischemic heart disease (IHD) is one of the major causes of death worldwide because it can trigger adverse cardiac remodelling leading to heart failure[1]. Myocardial ischemia exhibits imbalance between myocardial oxygen supply and demand caused by impediment of coronary blood flow by coronary stenosis, thrombosis, hyperconstriction of epicardial and microvascular coronary arteries thereby leading to reduced supply of myocardial oxygen[2]. Vascular complications of diabetes create a severe threat to human health. In people affected by diabetes, blood vessels of various types, including cardiac arteries and microvessels develop atherosclerosis and microvascular endothelial function impairment, basement membrane thickening, and microthrombosis. Cardiac microangiopathy coexist with macroangiopathy[3]. Moreover, diabetes compromises the potential for compensatory angiogenesis in ischemia [4]. Endothelial dysfunction significantly contributes to pathophysiology of microvascular disease [4,5]. Endothelial cells (ECs) play a pivotal role in reparative angiogenesis and in maintaining the cardiac functions [6,7]. Therefore, it is of great significance to identify factors and the underlying molecular mechanisms in the ECs which could aid in better therapeutic interventions in the context of human IHD and diabetes.

CircRNAs are single stranded, covalently bonded loop structures[8]. Their circular shape makes them very stable and resistant to exonucleases [9]. CircRNAs were initially detected in humans in 1993 and were considered as products of “mis-splicing” [10]. Later studies indicated their role as potential regulators of physiological functions [11,12]. In contrast to linear RNA, circRNAs are generated through back splicing that connects the exon towards the 3’ end to an exon at the 5’ end thus forming a circular structure[8].

This alteration in exon order provides a criterion for efficiently detecting back-spliced junctions during the alignment step in bioinformatics analyses [12]. CircRNAs have been implicated in indirect regulation of gene expression through their interaction with RNA-binding proteins (RBPs) and with microRNAs (miRNAs) as 'miRNA sponges' thus acting as post-transcriptional regulator of gene expression [13]. miRNAs are small non-coding RNAs, which are produced as double-stranded primary transcripts (pri-miRNA) and then trimmed by microprocessor complex into smaller double stranded precursor miRNAs (pre-miRNA), with a stem-loop structure called pre-miRNAs. Pre-miRNAs are further trimmed in the cytoplasm by Dicer producing two ~22nucleotide-long single stranded mature miRNAs (identified as -3p and -5p), which can become a part of RNA-induced silencing complex (RISC) that represses gene expression through semi-complementarity of the miRNA seed sequence with miRNA binding sites usually placed in the 3'-UTR of the mRNAs [14,15]. CircRNAs bind to miRNAs via multiple miRNA response elements (MRE) which makes the miRNAs unavailable to bind to and repress their targeted mRNAs [16]. This results in stability of target mRNAs hence upregulation of proteins.

Many circRNA identification and annotation tools are available [reviewed in [16]]. For accurate identification of circRNAs from sequencing data, it is important to reduce false-positive rate of detection of back spliced junction reads. This can be achieved by considering detection of these junctions in several samples to gain more confidence or by applying a strict threshold on number of reads mapping to these junctions [17]. Most circRNA identification tools depend on aligners such as Bowtie [18], BWA [19] and STAR [20]. Several circRNA identification programs are available including Find_circ (https://github.com/marvin-jens/find_circ), CIRI [21], CIRCexplorer [22], CircTest [23], KNIFE [24] etc. Among these CIRCexplorer and KNIFE achieved the best sensitivity in detecting circRNAs [25].

CircRNAs have been shown to regulate angiogenesis and EC response to ischemia/reperfusion (I/R) injury [26,27,28]. We have recently reviewed the RNA regulatory role of circRNAs in IHD and cardiac remodelling[29,30]. However, the circRNAs governing endothelial-relevant miRNA-mRNA networks in the human heart affected by IHD and T2DM remains largely unexplored.

To characterized clinically relevant heart circRNAs, miRNAs and mRNAs, this study has employed a reverse translational approach based on the use of clinical samples and patients' databases collected as part of a specifically designed prospectively observational study. We have applied an integrative approach involving bioinformatics and experimental validations in cultured cardiac cell models.

METHODS

ARCADIA sample collection

ARCADIA (Association of non-coding RNAs with CAD and type-2 Diabetes - -REC Number: 13/LO/1687) is an observational prospective cohort study developed between two-centres, the Bristol Royal Infirmary (University Hospitals Bristol NHS Foundation Trust) and the Hammersmith Hospital (Imperial College Healthcare NHS Trust). Written informed consent was obtained from all patients. All human samples were obtained in accordance with the principles of the Declaration of Helsinki. The study was reviewed and approved by the National Research Ethics Service Committee London–Fulham (date of approval, 20 Dec 2013; reference REC 13/LO/1687). A patient characteristics table is provided in the supplementary information.

ARCADIA sample processing

Left ventricular (LV) biopsies were taken from the apex of the heart using a biopsy needle. For detailed methods, see our published article [31]. Following collection, these were placed into RNA*later* (Ambion) and incubated overnight at 4°C. RNA*later* was removed, and sample frozen at -80°C.

RNA extraction from LV biopsies

RNA extraction from human LV biopsies was performed using the *mir*Vana kit (AM1560) following the manufacturer's protocol, with the exception that samples were eluted in 50 µL nuclease-free water See details in our published article [31].

RNA sequencing

RNA extracted from human left ventricular tissue was digested with DNase I (Invitrogen DNA-*free* DNA removal kit AM1906). 20 ng digested RNA was depleted of rRNA (NEBNext rRNA depletion kit E6350L), and libraries were constructed using the NEBNext Ultra II Directional RNA Library Prep Kit for Illumina (E7760S). The whole transcriptome libraries were sequenced on an Illumina HiSeq 2500 and small RNA-seq was carried out by Exiqon [31].

Bioinformatics analyses of RNA-sequencing data

The quality of sequenced data was assessed using the program FASTQC[32]. The quality of the small RNA library was found to be very good with mean quality Phred scores of over 30. There were no over-represented sequences. However, adaptor content was found which was trimmed before any subsequent analysis. The library size was estimated at 20 million reads and read length between 50 and 60 bp after removal of adaptors. The quality of sequenced data for the whole transcriptome library was equally good (mean quality Phred scores >30), except for one sample, which was found to have unusually high rRNA contamination. This sample was therefore excluded from downstream analyses. All the other samples showed no over-represented sequences or adaptor content. The library size was estimated at 70 million paired end reads with a read length of 100 bp. Samples that passed the QC step were aligned to the human genome (hg19) using the aligner STAR[20]. For long and small RNA libraries, raw read counts were generated using the R package Rsubread [33,34] and annotations were carried out using Ensembl GRCh37 (v75) and miRBase v20 respectively. Raw read counts were normalised using Trimmed Mean of M-values (TMM) method and differential expression (DE) calculated between the different groups using R package *Limma*[35]. CircRNAs were detected and annotated using CIRCexplorer[22] followed by normalisation (FPM) and DE analyses (R package *Limma*) (Supplementary Figure 1). FC and p-values were generated using *Limma*. P-value threshold of < 0.05 was used for finding DE circRNAs, miRNAs and mRNAs.

Prediction of circRNA-miRNA-mRNA networks

First, DE circRNAs (LV biopsies) were extracted to predict sponging interactions with miRNAs using three databases: TSCD (Tissue specific CircRNA database)[36], CSCD

(Cancer-Specific CircRNA Database)[37] and CRI (Circular RNA Interactome)[38] and the results were combined from all. Next, the sponged miRNAs were screened to keep only those with expression in the heart (LV biopsies). For these miRNAs, miRNA-mRNA interactions were predicted using miRWalk suite[39] and miRcode[40]. All interactions passing the threshold of binding probability (>0.95) were retained. Next, the mRNA targets were screened to keep only those with expression in the heart (LV biopsies). Following this, circRNA-miRNA-mRNA networks corresponding to IHD and IHD+T2DM were created by drawing the interactions in Cytoscape. Using published data on human ECs from Gene Expression Omnibus (GEO): GSE100242[41] (circRNAs, HUAECs), GSE53315[42] (miRNAs, HCAECs) and GSE134489[43] (mRNAs, HCAECs), we extracted all circRNAs, miRNAs and mRNAs from the networks that were expressed in ECs. Gene Ontology (GO) and KEGG pathway analysis was carried out using WebGestalt. Whereas GO provides information on the individual function of genes, KEGG is a collection of manually drawn pathways representing information of the molecular interaction between genes and reactions such as those in metabolic processes. KEGG pathways and GO biological processes that were significant with an FDR<0.05 were further examined.

Single cell and single nuclei RNA-sequencing data analysis

The raw data for single-nuclei and single-cell RNA sequencing from healthy donor hearts was acquired from human heart atlas (https://www.nature.com/articles/s41586-020-2797-4). The pseudo counts were calculated as the sum of Unique Molecular Identifier (UMIs) in cells of each cell-type from one donor and further normalized as counts per million (CPM). Boxplots were created to show the expression across different cell types, presented as log2-transformed CPM values. We also explored single nuclei data from the study of Koenig et al. (2022)[44]. In this study, a total of 26 control samples included 17 samples without diabetes and 9 samples with diabetes. We used this data to produce boxplots of expression in diabetes vs. non- diabetes samples.

Cell culture

Human cardiac microvascular ECs (HCMEC) and human umbilical vein ECs (HUVEC) were procured from PromoCell and cultured on 0.2 % gelatin (Sigma-Aldrich) in EGM2 (endothelial cell growth medium 2) medium (PromoCell). Human cardiac fibroblasts

(HCF) were procured from PromoCell as well and cultured in fibroblast growth medium 3 (PromoCell). Cells were used between passages 2 to 7 for the experiments. Proliferating AC16 human cardiomyocytes (Sigma-Aldrich SCC109, a gift from Professor Rajesh Katare, Otago University) were maintained in the basal media (DMEM/F-12 with 10% FBS, 1% L-Glutamine and 1% penicillin/streptomycin). Cell cultures were maintained at 37 °C in a humidified atmosphere containing 5% CO_2. For the induction of hypoxia (mimicking IHD), the cells were cultured for 48 hours in the presence of 1% O_2 at 37 °C in a humidified atmosphere containing 5% CO_2 and cultured in the presence of 25mM glucose for hypoxia and high glucose conditions (mimicking IHD and T2DM) respectively.

Transfection of Short Interfering RNA (siRNA) and Mimic miRNA

HCMECs or HUVECs were transfected with 30 nM of circNPHP1 siRNA or control siRNA (non-targeting negative control pool); hsa-miR-221-3p mimic or miRNA mimic negative control; anti-hsa-miR-221-3p or anti-miRNA negative control using Lipofectamine™ 2000 (ThermoFisher Scientific) for 48 hours, as previously described [45]. Details are provided in the major resources table.

BrdU Cell Proliferation Assay and apoptosis assay

HCMECs or HUVECs were seeded (1×10^4) in a 96-well plate and transfected with circNPHP1 siRNA or control siRNA. Cell proliferation was determined by BrdU (bromodeoxyuridine) incorporation using BrdU Cell Proliferation ELISA kit (Abcam) following manufacturer's instructions. Apoptosis was measured using RealTime-Glo™ Annexin V Apoptosis and Necrosis Assay kit (Promega) following manufacturer's instructions.

Endothelial Cord Formation Assay

HUVECs and HCMECs were transfected with circNPHP1 siRNA or control siRNA. 48 hours post-transfection, HUVECs (13×10^4) or HCMECs (15×10^4) were seeded on a 96-well plate coated with 50 µL Growth Factor Reduced Matrigel (Corning). After 8 hours of cord formation, plates were fixed with 4% formaldehyde followed by permeabilization with Triton X-100 and were stained with Phalloidin (Thermo Fischer Scientific). Images were captured at ×4 magnification using a *Zeiss Axio Observer*

inverted microscope. Angiogenesis was analyzed using the angiogenesis analyzer plugin for NIH ImageJ software.

RNA Isolation and Quantitative Real-Time Polymerase Chain Reaction (qPCR)

Total RNA was isolated from the cells using QIAzol reagent (Qiagen) following manufacturer's protocol. For gene expression analysis, cDNA was synthesized using the PrimeScript RT-PCR kit (Takara), according to the manufacturer's instructions. Quantitative real-time polymerase chain reaction (qPCR) was performed using TB Green Premix Ex Taq Kit (Takara) on QuantStudio 6 Flex Real-Time PCR System (Life Technologies). 18S rRNA (ribosomal RNA) was used for normalization.

For miRNAs analysis, cDNA was synthesized using miRCURY LNA RT Kit (Qiagen). Quantitative real-time polymerase chain reaction was performed using miRCURY LNA SYBR Green PCR Kit (Qiagen) following recommended instructions. Small RNA U6 was used for normalization.

For detection of circRNAs, divergent primers against the backsplice junction sequence were designed using NCBI Primer Design webtool. CircBase ID for circRNA candidates was identified according to the specific genomic coordinates. A 200nt long junction sequence, combining 100nt from the 3' end of the circRNA sequence to 100nt from the 5' end, was acquired using the Circular RNA Interactome webtool as the PCR amplicon sequence used for divergent primer design.

All the PCR primer sequences are listed in the major resources table.

CircRNA pull down assay

Pulldown of the circRNA was carried out according to the protocol described in [46]. Antisense oligo (ASO) probe 1 was designed by joining the last 15 nucleotides of circNPHP1 to the first 15 nucleotides to make a 30-nucleotide sequence against the backsplice junction followed by reverse complement. The second probe (probe 2) used to pulldown circNPHP1 consists of 22 nucleotide sequence against the backsplice junction, which is the siRNA sequence for circNPHP1 used in this study. Control ASO was chosen following the protocol. All the ASO probes were synthesized with biotin-TEG added to the 3' end of the sequences (Sigma-Aldrich). Briefly, 5 million cells were harvested in Tris, KCl, $MgCl_2$, nonidet P-40-polysome extraction buffer (PEB). Cell extracts were incubated with the 1 µl of biotinylated probes (100 µM) in Tris, EDTA, NaCl, Triton (TENT) buffer with rotation for 90 minutes at 4°C for

hybridization. Subsequently, streptavidin beads were washed in TENT buffer and added to the extracts and the probes and incubated with rotation for further 45 minutes at room temperature. Then the beads were washed thrice in TENT buffer followed by isolation of RNA using Trizol and phenol-chloroform. cDNA was synthesized and subjected to qPCR for determination of circNPHP1 and the bound miRNAs (described above). Fold enrichment was calculated in the pulldown samples with probe 1 and probe 2 against the control probe pulldown using delta delta Ct method (Livak). 18S and U6 were used as reference genes to normalize for circNPHP1, linear NPHP1 and miR-221-3p respectively.

The sequences of the probes are listed in the major resources table.

Western blot analysis

Cells were harvested and lysed in ice-cold RIPA buffer (Sigma-Aldrich) containing 1 mM orthovanadate, 1 mg/mL of protease inhibitor cocktail (Roche). Protein concentrations were determined using Bradford assay reagent (BIORAD). Equal amounts (15µg) of proteins were fractionated in 4-20 % SDS-polyacrylamide gel electrophoresis (SDS-PAGE) and transferred onto a polyvinylidene difluoride (PVDF) membrane using wet transfer method. The membranes were blocked with 5% milk followed by incubation with primary antibodies overnight using the following antibodies: anti-VEGF-A (Abcam), anti-BCL2 (Cell Signaling Technology), anti-Lamin B1 (Cell Signaling Technology). The membrane was further probed with anti-Rabbit IgG-HRP (Santa Cruz Biotechnology) and Immobilon Crescendo Western HRP substrate (Merck Millipore) was used to detect the chemiluminescence. Protein bands were visualized using the ChemiDoc™ MP Imaging System (BIORAD). Densitometry analysis of the gels was carried out using NIH ImageJ software. The details of antibodies are listed in the major resources table.

Statistical analysis

RNA-seq statistical analyses is detailed in section on bioinformatics analyses of RNAseq data.

For all other experiments, statistical analyses were performed with GraphPad Prism software (GraphPad). Normal distribution of each experimental group was determined by Shapiro-Wilk test. Statistical significance between two groups was analysed by unpaired Student *t* test. For the comparison between multiple groups, 1-way ANOVA

was performed and adjusted for multiple comparisons using post hoc Dunnett's test. Data are presented as mean±SEM. P values less than 0.05 were considered statistically significant.

RESULTS

Differentially expressed circRNAs, miRNAs and mRNAs in LV biopsy samples

Following RNA-seq analysis, we identified significantly DE circRNAs in IHD vs non-IHD, IHD+T2DM vs non-IHD and IHD+T2DM vs IHD respectively (Figure 2A, CircRNA identification pipeline: Supplementary Figure 1A). Additionally, number of detected circRNAs and their corresponding genes are shown in Supplementary Figure 1B and total DE circRNAs in Supplementary Figure 1C. We also identified: 1) miRNAs which were DE in IHD vs non-IHD, IHD+T2DM vs non-IHD and IHD+T2DM vs IHD, respectively (Figure 2B, Supplementary Figure 1C) and 2) mRNAs, which were DE in IHD vs non-IHD, IHD+T2DM vs non-IHD and IHD+T2DM vs IHD respectively (Figure 2C, Supplementary Figure 1C). As pathology of IHD includes coronary artery blockages as well as reduced vascularization and angiogenesis, we focussed on studying the circRNAs, miRNAs and mRNAs that might contribute to EC functions.

Significantly DE circRNAs are predicted to sponge miRs and affect their downstream mRNA targets in complex networks that are involved in EC-relevant pathways

After predicting interactions between circRNAs, miRNAs and mRNAs, networks were created in Cytoscape where the three types of RNAs were represented as points called "nodes" and interactions between them were represented by lines called "edges" that connect the points together. Three networks were created for the three comparisons: IHD vs non-IHD (305 nodes and 359 edges - Figure 3A, left), IHD+T2DM vs non-IHD (1046 nodes and 2803 edges - Figure 3B, left) and IHD+T2DM vs IHD (303 nodes and 361 edges - Figure 3C, left). The networks indicate putative regulatory relationships between circRNAs, miRNAs and mRNAs in the context of ECs as all 3 types of RNAs are expressed in ECs (using published data on ECs from GEO [see methods for details]). Following the network creation, it was imperative to identify the biological processes and pathways that these RNAs contributed to. For that we carried out GO and KEGG pathway analyses using tools given in methods. All processes and

pathways that were enriched in the network with FDR<0.05 were considered significant (Figure 3 A, B and C; right). These analyses resulted in the identification of biological processes and pathways such as VEGF signaling, angiogenesis, apoptosis and HIF-1 signaling which are of possible relevance for vascular biology and disease (highlighted in colors in Figure 3).

Validation of DE circRNAs that are predicted to be involved in angiogenesis and VEGF-A signalling

CircRNAs were selected from each network based on the EC-relevant enriched pathways such as angiogenesis and VEGF signalling (large red labelled nodes in Figure 3 A, B and C, left). These included circNPHP1 (Figure 3B and 3C), circMCU (Figure 3A), circSTX17 and circMGA (Figure 3C). After screening for the expressional changes induced by exposure of ECs to disease mimicking conditions, circNPHP1 emerged at the top out of 5 tested circRNA candidates identified from the bioinformatics analyses (Supplementary Figure 1D). We therefore confirmed the quantification of circNPHP1 in both HCMECs and HUVECs exposed to hypoxia and hypoxia+HG as compared to cells kept under standard culture conditions (Figure 4C) and demonstrating that the linear NPHP1 form was not affected by difference in culture conditions (Supplementary Figure 3A). These data obtained in ECs exposed to disease-mimicking conditions were aligned with the results of qRT-PCR analyses in LV (N=5 biological replicates per groups) (Figure 4B). As shown in Figure 4A, LV RNA-seq analyses (N=12 biological replicates per groups) identified the levels of circNPHP1 (chr2:110919179-110920709) to be increased in both IHD+T2DM vs non-IHD (Log2FC 0.95; Pvalue 0.043) and IHD+T2DM vs IHD (LogFC 1.2; P value 0.027) (Figure 4A, left) whereas its linear counterpart remains unchanged (Figure 4A, right). We next used single-cell and single-nuclei RNAseq data from heart atlas (Supplementary Figure 2A) to investigate whether circNPHP1 expression is confined to EC or present in different cell types of the human heart. Because traditional scRNA-seq does not allow for circRNA identification, we resolved to search for the linear NPHP1 form under the assumption that cells expressing linear NPHP1 would be capable to produce its circular counterparts. Our analyses identified NPHP1 to be ubiquitously expressed in different heart cells (Supplementary Figure 2B). Using single nuclei data from Koenig et al[44], we show that expression levels of linear NPHP1 do not change between diabetic and healthy controls.

CircNPHP1 promotes proliferation and angiogenesis in the ECs

To investigate the functional relevance of circNPHP1 for the human endothelium, HUVECs and HCMECs were transfected with circNPHP1 siRNA or control siRNA and submitted to EC biology tests (cell proliferation, apoptosis, and angiogenesis) performed under normal, hypoxia and hypoxia+HG conditions. Knockdown of circNPHP1 specifically downregulated the circular form whereas linear NPHP1 remained unchanged elucidating the specificity of the siRNA for the circular form of NPHP1 (Supplementary Figure 3A).

Silencing by circNPHP1 siRNA in the HCMECs and HUVECs, markedly reduced the cell proliferation as measured by BrDU incorporation across all the conditions (Figure 5A). Apoptotic activity of the cells remained unaffected upon circNPHP1 knockdown as observed in HCMECs (Figure 5B). Upon circNPHP1 knockdown in the HUVECs and HCMECs, cord formation assay on matrigel showed prominent reduction of angiogenesis. The total tube length and the number of branches, meshes, nodes, junctions exhibited significant reduction (Supplementary Figure 3B, 3C and Figure 5C).

Additionally, in hypoxia and hypoxia+HG conditions, similar reduction of angiogenesis was observed in HUVECs upon silencing circNPHP1 (Figure 5C). Altogether our results strongly support circNPHP1 to be involved in promoting proliferation and angiogenesis in the ECs.

CircNPHP1 binds to and sponges miR-221-3p in ECs

Extracting the sub-network of circNPHP1 from T2DM network, we found 9 miRNA candidates predicted to be sponged by circNPHP1 and 38 mRNAs predicted to be targeted by these miRNAs (Figure 6A, left). GO and KEGG pathway analyses was carried out using the tools mentioned in methods. Significantly enriched biological processes and pathways (FDR<0.05) included angiogenesis, VEGF signalling, HIF1 signalling, chromatin remodelling etc. which indicates that circNPHP1 might be involved in various pathways through a combination of miRNA and mRNA partners.

To validate the predicted interactions of the identified miRNAs with circNPHP1, pulldown of circNPHP1 was carried out in the HUVECs by using either probe 1, which is a 30-nucleotides ASO probe designed against the sequence of its backsplice junction, or probe 2, which is a ASO probe including the siRNA sequence contained in the backsplice junction (Supplementary Figure 4A) (see details of probes in

methods). The pull-down of circNPHP1 by each probe and the enrichment of the miRNAs was investigated using qRT-PCR. The results showed effective enrichment of circNPHP1 pulldown by either probe (Figure 6B). Among the predicted circNPHP1-sponged miRNAs, we found only miR-221-3p to be effectively enriched in the pull-down (Supplementary Figure 4B and Figure 6B). Of note, the miR-221-3p enrichment was effective in the case of probe 2 but not in probe 1. A possible explanation could be steric hindrance in binding of miR-221-3p caused by other factors bound to probe1 due to larger size. Additionally, knockdown of circNPHP1 abolished the enrichment of miR-221-3p by the probes, further augmenting the evidence of binding of miR-221-3p to circNPHP1 (Figure 6C). The linear form of NPHP1 was only detectable in the whole cell extracts and was undetermined by qRT-PCR in the corresponding circNPHP1 enriched conditions, indicating specific pulldown of the circular RNA (Supplementary Figure 4C). To investigate if the putative circNPHP1/miR-221-axis was relevant to other cardiac cell types, we first measured the expression of both RNA molecules by qRT-PCR in human AC16 (left ventricle cardiomyocyte cell line) and human cardiac fibroblasts, before proceeding with the circNPHP1 pull-down experiment. Expression of circNPHP1 and miR-221-3p in AC16 was well-detected and comparable to HUVECs (ct: 30 for circNPHP1 and ct: 19 for mir-221-3p). Although miR-221-3p exhibited good expression (ct: 25) in the cardiac fibroblasts, the expression of circNPHP1 as well as the linear form was poor (ct: 35) (Supplementary Figure 4D). In AC16, probe 2 induced effective pulldown of circNPHP1, which was associated with enrichment of miR-221-3p (Supplementary Figure 4E). We also found some enrichment of miR-221-3p in cardiac fibroblasts but the pulldown of circNPHP1 by either probe 1 or probe 2 was not effective due to low expression of circNPHP1 (Supplementary Figure 4F). Interestingly, the proliferation of cardiac fibroblasts significantly decreased upon silencing circNPHP1 (Supplementary Figure 5A) whereas the cellular apoptosis in cardiac fibroblasts and AC16 remained unchanged (Supplementary Figure 5B). Together, our data suggests that the circNPHP1/ miR-221-3p axis is operational in difference cell types and could mediate different responses.

CircNPHP1 levels influences the expression of miR-221-3p targets (BCL2 and VEGFA) in ECs

To confirm that sponging of miR221-3p by circNPHP1 prevents the miRNA from repressing target mRNAs, we focussed on three direct targets of miR221-3p (BCL2, BCL2L11 (BIM) and VEGFA) [47,48,49,50], which were also predicted to influence angiogenesis and cell survival based on our pathway analyses . We first validated that miR-221-3p mimic repressed VEGFA and BCL2 expression while anti-miR-221-3p increased their expression in HUVECs. BIM was unaffected in both cases (Supplementary Figure 6A and 6B). Next, HUVECs were transfected with either circNPHP1 siRNA or control siRNA and cultured under hypoxia and hypoxia+HG conditions. Silencing of circNPHP1 downregulated VEGFA and BCL2 mRNA levels in normal, hypoxia and hypoxia + HG conditions. Expression of BIM remained unchanged (Figure 7A) and hence excluded from further analyses. The protein levels of VEGF-A and BCL2 showed significant reduction upon silencing of circNPHP1 under normal and disease mimicking conditions (Figure 7B). To further assess any additive effect of circNPHP1 and miR221-3p, HUVECs were transfected with circNPHP1 siRNA or control siRNA in combination with miR221-3p mimic. Silencing of circNPHP1 and overexpression of miR221-3p significantly decreased VEGFA and BCL2 mRNA levels. Further reduction of mRNA expression as a combinatorial effect was not observed (Figure 7C). However, the inhibitory effect of circNPHP1 silencing on BCL2 and VEGFA was reduced when ECs were treated with an anti-miR221-3p together with circNPHP1 siRNA further confirming the joint operation of circNPHP1 and miR-221-3p in regulating VEGFA and BCL2 (Figure 7D).

DISCUSSION

Identifying biological mediators of IHD can vastly improve the understanding of its pathogenicity at a molecular level and help develop new therapies for its treatment. Despite advancement in research to gain an understanding of circRNAs and their role in sponging of miRNAs, the interactions between different RNA species are largely unexplored in human IHD. We present here, for the first time, regulatory networks involving circRNAs, miRNAs and mRNAs in IHD. Specifically, we identified circRNAs from whole transcriptome sequencing by putting together a pipeline using STAR and CIRCexplorer to detect back-spliced junctions. We also identified mRNAs and

miRNAs from our whole transcriptome and small RNA sequencing data respectively. Following detection of the various RNA species and performing differential expression (DE) analysis, we used streamlined bioinformatics approaches to construct circRNA-miRNA-mRNA networks in IHD and IHD+T2DM with a particular focus on EC biology and processes (angiogenesis, apoptosis, proliferation). Our study provides unique information on the putative interactions between these three RNA species (circRNA, miRNA and mRNA) in IHD with/out T2DM and is a useful resource for developing testable hypothesis for future therapeutic studies. Our study highlights a novel proangiogenic subnetwork commanded by circNPHP1, and its mechanisms in IHD and T2DM.

The role of circRNAs as sponges of miRNAs and their implication in disease has been studied in the context of atherosclerosis[51,52], myocardial infarction[53],cardiac fibrosis, cardiac hypertrophy[54], heart failure[55] and cardiac senescence[56] with ischemic heart disease still relatively less studied[57]. CircSLC8A1, which is enriched in cardiomyocytes, was reported as the most abundant circRNA in the human heart[58]. CircRNAs are also implicated as potential candidates for the treatment of cardiac fibrosis [27,59,60.] A recent study reported 662 circRNA-miRNA-mRNA interactions in heart failure patients[61]. Previous studies have demonstrated the associations between T2DM and circRNAs in diabetic cardiomyopathy. These include circRNA_000203 (MYO9A), circRNA_010567 (CDR1), and circHIPK3 which are increased in diabetic mice and promote myocardial fibrosis [62, 63, 64]. We also checked the levels of these circRNAs in our LV biopsy datasets and found circSLC8A1 and circHIPK3 to be increased in IHD and IHD with T2DM as compared to non-IHD patients whereas circMYO9A does not change and CDR1 was not detectable.

We identified few circRNA candidates from each network based on pathway analysis with a particular focus on terms relevant to EC biology and angiogenesis. Out of the 4 tested circRNAs, circNPHP1 was found to increase in ECs cultured under disease mimicking conditions as compared to controls. To date, circNPHP1 has not been studied in cardiovascular disease. CircNPHP1 is derived from exons 9 and 10 of NPHP1 gene. Although other isoforms of the circular RNA were identified from our clinical samples (RNAseq), their expression was scarce or represented in very few samples. The linear NPHP1 transcript is uniformly expressed in the healthy and

diseased heart as evidenced from our RNAseq on heart LV biopsies and confirmed by single nuclei RNA-seq analyses, which indicated its expression to be ubiquitous, even if the binding partners and function might vary across different cell types. NPHP1 encodes for the protein *Nephrocystin 1* that was initially discovered to be localized to the primary cilia and apical surface of kidney epithelial cells and interacts with molecules that take part in cell adhesion, signalling and maintenance[65]. NPHP1 has been associated to kidney disease (nephronophthisis) caused due to autosomal recessive whole gene deletions resulting in abnormal structure and function of primary cilia [66]. In nephronophthisis patients, cardiac defects like septal and aortic valve anomalies have also been reported [67]. The direct involvement of NPHP1 in heart disease has not been reported to date and information from GWAS Catalog (EMBL-EBI; https://www.ebi.ac.uk/gwas/) indicates no involvement in CAD or T2DM. Worth noting is the fact that although levels of NPHP1 do not vary between IHD with/without T2DM and non-IHD patients (also confirmed by single-nuclei data), they vary quite significantly for one of the circular isoforms of this gene (circNPHP1, studied here). We found that although circNPHP1 levels are significantly upregulated in IHD with T2DM as compared to IHD and controls, the levels are not as distinct between IHD and controls (RNAseq). In qRT-PCR, we see upregulation of circNPHP1 in both IHD with and without T2DM as compared to controls. This can be attributed to variability in the samples and technical differences between the two methods. The findings of qRT-PCR are in line with data collected from ECs cultured under disease mimicking conditions. The linear form of NPHP1 remains unchanged between groups, as also indicated by single nuclei data in endothelial cells resident in diabetic and non-diabetic heart donors.

We found circNPHP1 to be strongly involved in promoting EC proliferation and angiogenesis under IHD and IHD+T2DM conditions. Previously, a few circRNAs have been reported to modulate angiogenesis such as CircFndc3b that modulates cardiac repair after myocardial infarction by promoting angiogenesis in the ECs through increased VEGF-A expression[53]. Extracellular vesicle-derived circCEBPZOS promotes angiogenesis and proliferation of cardiac ECs helping in cardiac repair[68]. Moreover, circZfp292 depletion reportedly abolishes laminar flow-induced alterations in EC orientation contributing to aberrant flow alignment in the aorta in vivo[69]. Finally, in senescent in mouse aortic ECs, circGSE1 promotes an angiogenic response [70].

However, in the context of human IHD and EC biology, the presence, interactions and functions of circRNAs remain largely unexplored.

Using our streamlined bioinformatics pipeline involving integration of different types of data including expression profiles of circRNA, miRNAs, mRNAs, published EC data, predictions on possible interactions between the three, mapping of biological processes and pathways, we extracted a novel proangiogenic subnetwork commanded by circNPHP1 along with its predicted sponged miRNA partners (n=9) and their downstream mRNA targets (n=38). To confirm the interaction of the identified miRNAs with circNPHP1, pulldown of circNPHP1 was carried out in HUVECs by using antisense oligo probes (probe 1 and 2) designed against the sequence of its backsplice junction [46,71]. Among the predicted miRNAs, we found only miR-221-3p to be effectively enriched. Although we predicted miR-222-3p as well which is highly homologous to miR-221-3p and encoded in tandem from a gene cluster and often operating together[72]; we did not observe enrichment in miR-222-3p. Although the pulldown of circNPHP1 with probe 1 was effective in the ECs, the enrichment of miR-221-3p with probe 1 was poor unlike significant enrichment with probe 2. This could be explained considering that probe 1 has a larger size which might bind other factors and can cause steric hindrance in binding of miR-221-3p. Additionally, circRNAs can possess certain conformational states which might confer differential binding to various factors[73].

In the proangiogenic subnetwork of circNPHP1, miR-221-3p was found to interact with BCL2 and VEGFA, which are both involved in angiogenesis [74,75] and BIM (BCL2L11) that works together with BCL2 in a context-dependent manner. miR-221-3p expression was already reported to be elevated in the rat post-MI [47,72]. miR-221-3p targets hypoxia inducible factor-1α (HIF-1α) to inhibit angiogenesis and its inhibition improves cardiac function in mouse heart failure model [47]. Additionally, miR-221-3p targeting of Ang-2 was reported to impair the proliferation and cord formation capacities of hypoxic human coronary microvascular ECs and to inhibit the formation of tip cells, which play a vanguard role in angiogenesis[49]. In apparent contrast with these and our data, miR-221-3p was proposed to promote the proangiogenic and wound healing properties exerted by endothelial progenitor cell-derived exosome and to increase VEGF expression[76]. VEGFA has long been established to play a

therapeutic proangiogenic roles in cardiac repair in IHD[77,78, 74]. On the other hand, BCL2 also plays a crucial role in regulating the mitochondrial oxidative stress and angiogenesis in IHD[75] and rat heart failure[79]. Our results in ECs confirmed that endogenous circNPHP1 dictates VEGFA and BCL2 expression by sponging miR-221-3p. By contrast, BIM which is largely pro-apoptotic [80,81] was unaffected upon modulation of circNPHP1.

We further investigated whether the circNPHP1/miR-221-3p axis is operational in other cell types. We also checked the binding of circNPHP1 to miR-221-3p in AC16 cell line (cardiomyocyte) and human cardiac fibroblasts. In AC16, probe 1 was not efficient in pulldown of circNPHP1 unlike ECs possibly due to differential binding of other factors. Similar to what was observed in the ECs, the enrichment of miR-221-3p was much more effective with probe 2. The expression of linear and circNPHP1 in AC16 is comparable to that of the ECs. Additionally, we also observed enrichment in miR-221-3p for both the probes in cardiac fibroblasts but the expression of both linear and circNPHP1 is very low and effective pulldown of circNPHP1 was not achieved by both the probes. Although cardiac fibroblasts have low expression of circNPHP1, we observed circNPHP1 to be profibrotic. We observed significant reduction in proliferation of cardiac fibroblasts upon silencing of circNPHP1 indicating its involvement in fibrosis. Both proliferation and apoptosis were unaffected in AC16 after silencing of circNPHP1 suggesting that the circNPHP1/miR221-3p is functional is regulating other phenotypes. Together, these results implicate that circNPHP1/miR-221-3p axis is potentially operational in different cardiac cell types. Its role in regulating distinct cell phenotypes needs further investigation.

As with any study, there are some limitations. One being that the number of biopsy samples is relatively small therefore the findings of this study must be replicated in other human patient cohorts. Another limitation is the scarcity of available cell-level data particularly for circRNAs, which suffers from the fact that scRNA-seq datasets are produced with methodologies that have biases to detect abundant transcripts, have a low sequencing coverage and low capture efficiency. These limitations make it difficult to extract circRNAs. Finally, we have focussed on EC and future studies should be dedicated to exploit the circRNA-miRNA-mRNA circuits identified with this study.

In conclusion, our study has identified novel differential circRNA-miRNA-mRNA networks in IHD and IHD+T2DM with a particular focus on ECs. It specifically highlights the proangiogenic axis involving circNPHP1/miR-221-3p/VEGFA/BCL2 in IHD and IHD+T2DM implicating its potential significance for therapeutic angiogenesis and cardiac repair.

ACKNOWLEDGEMENTS

We are grateful to Dr. Fabio Martelli and Dr. Alessia Bibi for critical discussions and advice regarding the circRNA pulldown experiments. We are also thankful to Prof. Pilar Ruiz-Lozano, Dr. Hassan Abdulrazzak and Junqing Zhang for providing HCMECs and human cardiac fibroblasts; Dr. Walid Sweaad, Dr. Pragati Panday, Junyi Liu and Casey Lau for general support with this study. Dr Cristina Beltrami supported us in the initial phase of the ARCADIA sample collection. Panagiotis Kyriazis (Imperial College) and several Bristol clinical trial unit staff supported us for the administrative aspects of the ARCADIA study. We are also grateful to the patients, surgeons and research nurses and Bristol clinical trial unit staff who contribute into the ARCADIA studies and to the British Heart Foundation and UK National Institute of heart Research (NIHR) for funding this research. For illustrations, we used some images from Vecteezy (www.vecteezy.com).

SUPPLEMENTARY DATA

Patient characteristics ARCADIA study

Major resources table

REFERENCES

1. Crossman, D.C. The pathophysiology of myocardial ischaemia. *Heart* **90**, 576-580 (2004).
2. Shimokawa, H. & Yasuda, S. Myocardial ischemia: current concepts and future perspectives. *J Cardiol* **52**, 67-78 (2008).
3. Rask-Madsen, C. & King, G.L. Vascular complications of diabetes: mechanisms of injury and protective factors. *Cell Metab* **17**, 20-33 (2013).
4. Severino, P.*, et al.* Diabetes Mellitus and Ischemic Heart Disease: The Role of Ion Channels. *Int J Mol Sci* **19**(2018).

5. Sinha, A., Rahman, H. & Perera, D. Coronary microvascular disease: current concepts of pathophysiology, diagnosis and management. *Cardiovasc Endocrinol Metab* **10**, 22-30 (2021).
6. Talman, V. & Kivela, R. Cardiomyocyte-Endothelial Cell Interactions in Cardiac Remodeling and Regeneration. *Front Cardiovasc Med* **5**, 101 (2018).
7. Pinto, A.R.*, et al.* Revisiting Cardiac Cellular Composition. *Circ Res* **118**, 400-409 (2016).
8. Tang, X.*, et al.* Review on circular RNAs and new insights into their roles in cancer. *Comput Struct Biotechnol J* **19**, 910-928 (2021).
9. Chen, L.L. & Yang, L. Regulation of circRNA biogenesis. *RNA Biol* **12**, 381-388 (2015).
10. Cocquerelle, C., Mascrez, B., Hetuin, D. & Bailleul, B. Mis-splicing yields circular RNA molecules. *FASEB J* **7**, 155-160 (1993).
11. Jeck, W.R.*, et al.* Circular RNAs are abundant, conserved, and associated with ALU repeats. *RNA* **19**, 141-157 (2013).
12. Jeck, W.R. & Sharpless, N.E. Detecting and characterizing circular RNAs. *Nat Biotechnol* **32**, 453-461 (2014).
13. Barrett, S.P. & Salzman, J. Circular RNAs: analysis, expression and potential functions. *Development* **143**, 1838-1847 (2016).
14. O'Brien, J., Hayder, H., Zayed, Y. & Peng, C. Overview of MicroRNA Biogenesis, Mechanisms of Actions, and Circulation. *Front Endocrinol (Lausanne)* **9**, 402 (2018).
15. Gregory, R.I.*, et al.* The Microprocessor complex mediates the genesis of microRNAs. *Nature* **432**, 235-240 (2004).
16. Panda, A.C. Circular RNAs Act as miRNA Sponges. *Adv Exp Med Biol* **1087**, 67-79 (2018).
17. Szabo, L. & Salzman, J. Detecting circular RNAs: bioinformatic and experimental challenges. *Nat Rev Genet* **17**, 679-692 (2016).
18. Langmead, B., Trapnell, C., Pop, M. & Salzberg, S.L. Ultrafast and memory-efficient alignment of short DNA sequences to the human genome. *Genome Biol* **10**, R25 (2009).
19. Li, H. & Durbin, R. Fast and accurate short read alignment with Burrows-Wheeler transform. *Bioinformatics* **25**, 1754-1760 (2009).
20. Dobin, A.*, et al.* STAR: ultrafast universal RNA-seq aligner. *Bioinformatics* **29**, 15-21 (2013).
21. Gao, Y., Wang, J. & Zhao, F. CIRI: an efficient and unbiased algorithm for de novo circular RNA identification. *Genome Biol* **16**, 4 (2015).
22. Ma, X.K., Xue, W., Chen, L.L. & Yang, L. CIRCexplorer pipelines for circRNA annotation and quantification from non-polyadenylated RNA-seq datasets. *Methods* **196**, 3-10 (2021).
23. Cheng, J., Metge, F. & Dieterich, C. Specific identification and quantification of circular RNAs from sequencing data. *Bioinformatics* **32**, 1094-1096 (2016).
24. Szabo, L.*, et al.* Statistically based splicing detection reveals neural enrichment and tissue-specific induction of circular RNA during human fetal development. *Genome Biol* **16**, 126 (2015).
25. Zeng, X., Lin, W., Guo, M. & Zou, Q. A comprehensive overview and evaluation of circular RNA detection tools. *PLoS Comput Biol* **13**, e1005420 (2017).
26. Xiong, J., Hu, Y., Liu, Y. & Zeng, X. CircRNA mmu_circ_0000021 regulates microvascular function via the miR-143-3p/NPY axis and intracellular calcium following ischemia/reperfusion injury. *Cell Death Discov* **8**, 315 (2022).

27. Yang, T.*, et al.* Circle the Cardiac Remodeling With circRNAs. *Front Cardiovasc Med* **8**, 702586 (2021).
28. Long, Q., Lv, B., Jiang, S. & Lin, J. The Landscape of Circular RNAs in Cardiovascular Diseases. *Int J Mol Sci* **24**(2023).
29. Caporali, A.*, et al.* Non-coding RNAs as therapeutic targets and biomarkers in ischaemic heart disease. *Nat Rev Cardiol* (2024).
30. Bibi, A.e.a. Circular RNA regulatory role in pathological cadiac remodeling. *BJP* **DOI:10.1111/bph.16434**(2024).
31. Ford, K.L.*, et al.* Optimisation of laboratory methods for whole transcriptomic RNA analyses in human left ventricular biopsies and blood samples of clinical relevance. *PLoS One* **14**, e0213685 (2019).
32. S., A. FastQC: A Quality Control tool for High Throughput Sequence Data. in *http://www.bioinformatics.babraham.ac.uk/projects/fastqc* (2014).
33. Liao, Y., Smyth, G.K. & Shi, W. featureCounts: an efficient general purpose program for assigning sequence reads to genomic features. *Bioinformatics* **30**, 923-930 (2014).
34. Liao, Y., Smyth, G.K. & Shi, W. The Subread aligner: fast, accurate and scalable read mapping by seed-and-vote. *Nucleic Acids Res* **41**, e108 (2013).
35. Robinson, M.D. & Oshlack, A. A scaling normalization method for differential expression analysis of RNA-seq data. *Genome Biol* **11**, R25 (2010).
36. Xia, S.*, et al.* Comprehensive characterization of tissue-specific circular RNAs in the human and mouse genomes. *Brief Bioinform* **18**, 984-992 (2017).
37. Xia, S.*, et al.* CSCD: a database for cancer-specific circular RNAs. *Nucleic Acids Res* **46**, D925-D929 (2018).
38. Dudekula, D.B.*, et al.* CircInteractome: A web tool for exploring circular RNAs and their interacting proteins and microRNAs. *RNA Biol* **13**, 34-42 (2016).
39. Sticht, C., De La Torre, C., Parveen, A. & Gretz, N. miRWalk: An online resource for prediction of microRNA binding sites. *PLoS One* **13**, e0206239 (2018).
40. Jeggari, A., Marks, D.S. & Larsson, E. miRcode: a map of putative microRNA target sites in the long non-coding transcriptome. *Bioinformatics* **28**, 2062-2063 (2012).
41. Maass, P.G.*, et al.* A map of human circular RNAs in clinically relevant tissues. *J Mol Med (Berl)* **95**, 1179-1189 (2017).
42. Tabet, F.*, et al.* HDL-transferred microRNA-223 regulates ICAM-1 expression in endothelial cells. *Nat Commun* **5**, 3292 (2014).
43. Jung, H.S.*, et al.* TNF-alpha induces acyl-CoA synthetase 3 to promote lipid droplet formation in human endothelial cells. *J Lipid Res* **61**, 33-44 (2020).
44. Koenig, A.L.*, et al.* Single-cell transcriptomics reveals cell-type-specific diversification in human heart failure. *Nat Cardiovasc Res* **1**, 263-280 (2022).
45. Chamorro-Jorganes, A.*, et al.* METTL3 Regulates Angiogenesis by Modulating let-7e-5p and miRNA-18a-5p Expression in Endothelial Cells. *Arterioscler Thromb Vasc Biol* **41**, e325-e337 (2021).
46. Das, D., Das, A. & Panda, A.C. Antisense Oligo Pulldown of Circular RNA for Downstream Analysis. *Bio Protoc* **11**, e4088 (2021).
47. Li, Y., Yan, C., Fan, J., Hou, Z. & Han, Y. MiR-221-3p targets Hif-1alpha to inhibit angiogenesis in heart failure. *Lab Invest* **101**, 104-115 (2021).
48. Zhao, L. & Pan, Q. Highly-Expressed MiR-221-3p Distinctly Increases the Incidence of Diabetic Retinopathy in Patients With Type 2 Diabetes Mellitus. *Transl Vis Sci Technol* **12**, 17 (2023).

49. Yang, P., Yang, Q., Yang, Y., Tian, Q. & Zheng, Z. miR-221-3p targets Ang-2 to inhibit the transformation of HCMECs to tip cells. *J Cell Mol Med* **27**, 3247-3258 (2023).
50. Di Martino, M.T.*, et al.* miR-221/222 as biomarkers and targets for therapeutic intervention on cancer and other diseases: A systematic review. *Mol Ther Nucleic Acids* **27**, 1191-1224 (2022).
51. Song, C.L.*, et al.* Effect of Circular ANRIL on the Inflammatory Response of Vascular Endothelial Cells in a Rat Model of Coronary Atherosclerosis. *Cell Physiol Biochem* **42**, 1202-1212 (2017).
52. Cao, Q., Guo, Z., Du, S., Ling, H. & Song, C. Circular RNAs in the pathogenesis of atherosclerosis. *Life Sci* **255**, 117837 (2020).
53. Garikipati, V.N.S.*, et al.* Circular RNA CircFndc3b modulates cardiac repair after myocardial infarction via FUS/VEGF-A axis. *Nat Commun* **10**, 4317 (2019).
54. Wang, K.*, et al.* A circular RNA protects the heart from pathological hypertrophy and heart failure by targeting miR-223. *Eur Heart J* **37**, 2602-2611 (2016).
55. Wang, Y.*, et al.* A novel identified circular RNA, circSnap47, promotes heart failure progression via regulation of miR-223-3p/MAPK axis. *Mol Cell Biochem* **478**, 459-469 (2023).
56. Du, W.W.*, et al.* Foxo3 circular RNA promotes cardiac senescence by modulating multiple factors associated with stress and senescence responses. *Eur Heart J* **38**, 1402-1412 (2017).
57. Tian, M.*, et al.* CircSLC8A1 and circNFIX can be used as auxiliary diagnostic markers for sudden cardiac death caused by acute ischemic heart disease. *Sci Rep* **11**, 4695 (2021).
58. Lim, T.B.*, et al.* Targeting the highly abundant circular RNA circSlc8a1 in cardiomyocytes attenuates pressure overload induced hypertrophy. *Cardiovasc Res* **115**, 1998-2007 (2019).
59. Yu, Z., Huang, Q., Zhang, Q., Wu, H. & Zhong, Z. CircRNAs open a new era in the study of cardiovascular disease (Review). *Int J Mol Med* **47**, 49-64 (2021).
60. Gupta, S.K.*, et al.* Quaking Inhibits Doxorubicin-Mediated Cardiotoxicity Through Regulation of Cardiac Circular RNA Expression. *Circ Res* **122**, 246-254 (2018).
61. Made, A.*, et al.* circRNA-miRNA-mRNA Deregulated Network in Ischemic Heart Failure Patients. *Cells* **12**(2023).
62. Fan, W., Pang, H., Xie, Z., Huang, G. & Zhou, Z. Circular RNAs in diabetes mellitus and its complications. *Front Endocrinol (Lausanne)* **13**, 885650 (2022).
63. Yuan, L., Duan, J. & Zhou, H. Perspectives of circular RNAs in diabetic complications from biological markers to potential therapeutic targets (Review). *Mol Med Rep* **28**(2023).
64. Sakshi, S., Jayasuriya, R., Ganesan, K., Xu, B. & Ramkumar, K.M. Role of circRNA-miRNA-mRNA interaction network in diabetes and its associated complications. *Mol Ther Nucleic Acids* **26**, 1291-1302 (2021).
65. Salomon, R., Saunier, S. & Niaudet, P. Nephronophthisis. *Pediatr Nephrol* **24**, 2333-2344 (2009).
66. Leggatt, G.*, et al.* A genotype-to-phenotype approach suggests under-reporting of single nucleotide variants in nephrocystin-1 (NPHP1) related disease (UK 100,000 Genomes Project). *Sci Rep* **13**, 9369 (2023).

67. Pierpont, M.E., *et al.* Genetic Basis for Congenital Heart Disease: Revisited: A Scientific Statement From the American Heart Association. *Circulation* **138**, e653-e711 (2018).
68. Yu, L., *et al.* Extracellular vesicle-derived circCEBPZOS attenuates postmyocardial infarction remodeling by promoting angiogenesis via the miR-1178-3p/PDPK1 axis. *Commun Biol* **6**, 133 (2023).
69. Heumuller, A.W., *et al.* Locus-Conserved Circular RNA cZNF292 Controls Endothelial Cell Flow Responses. *Circ Res* **130**, 67-79 (2022).
70. Qiu, J., *et al.* Circular RNA circGSE1 promotes angiogenesis in ageing mice by targeting the miR-323-5p/NRP1 axis. *Aging (Albany NY)* **14**, 3049-3069 (2022).
71. Pandey, P.R., *et al.* Methods for analysis of circular RNAs. *Wiley Interdiscip Rev RNA* **11**, e1566 (2020).
72. Song, J., *et al.* Potential Value of miR-221/222 as Diagnostic, Prognostic, and Therapeutic Biomarkers for Diseases. *Front Immunol* **8**, 56 (2017).
73. Sun, H., *et al.* CircRNA May Not Be "Circular". *Front Genet* **12**, 633750 (2021).
74. Braile, M., *et al.* VEGF-A in Cardiomyocytes and Heart Diseases. *Int J Mol Sci* **21**(2020).
75. Uraoka, M., *et al.* Loss of bcl-2 during the senescence exacerbates the impaired angiogenic functions in endothelial cells by deteriorating the mitochondrial redox state. *Hypertension* **58**, 254-263 (2011).
76. Xu, J., *et al.* miRNA-221-3p in Endothelial Progenitor Cell-Derived Exosomes Accelerates Skin Wound Healing in Diabetic Mice. *Diabetes Metab Syndr Obes* **13**, 1259-1270 (2020).
77. Gogiraju, R., Bochenek, M.L. & Schafer, K. Angiogenic Endothelial Cell Signaling in Cardiac Hypertrophy and Heart Failure. *Front Cardiovasc Med* **6**, 20 (2019).
78. Collen, A., *et al.* VEGFA mRNA for regenerative treatment of heart failure. *Nat Rev Drug Discov* **21**, 79-80 (2022).
79. Siltanen, A., *et al.* Bcl-2 improves myoblast sheet therapy in rat chronic heart failure. *Tissue Eng Part A* **17**, 115-125 (2011).
80. Gogada, R., *et al.* Bim, a proapoptotic protein, up-regulated via transcription factor E2F1-dependent mechanism, functions as a prosurvival molecule in cancer. *J Biol Chem* **288**, 368-381 (2013).
81. Koenig, M.N., *et al.* Pro-apoptotic BIM is an essential initiator of physiological endothelial cell death independent of regulation by FOXO3. *Cell Death Differ* **21**, 1687-1695 (2014).

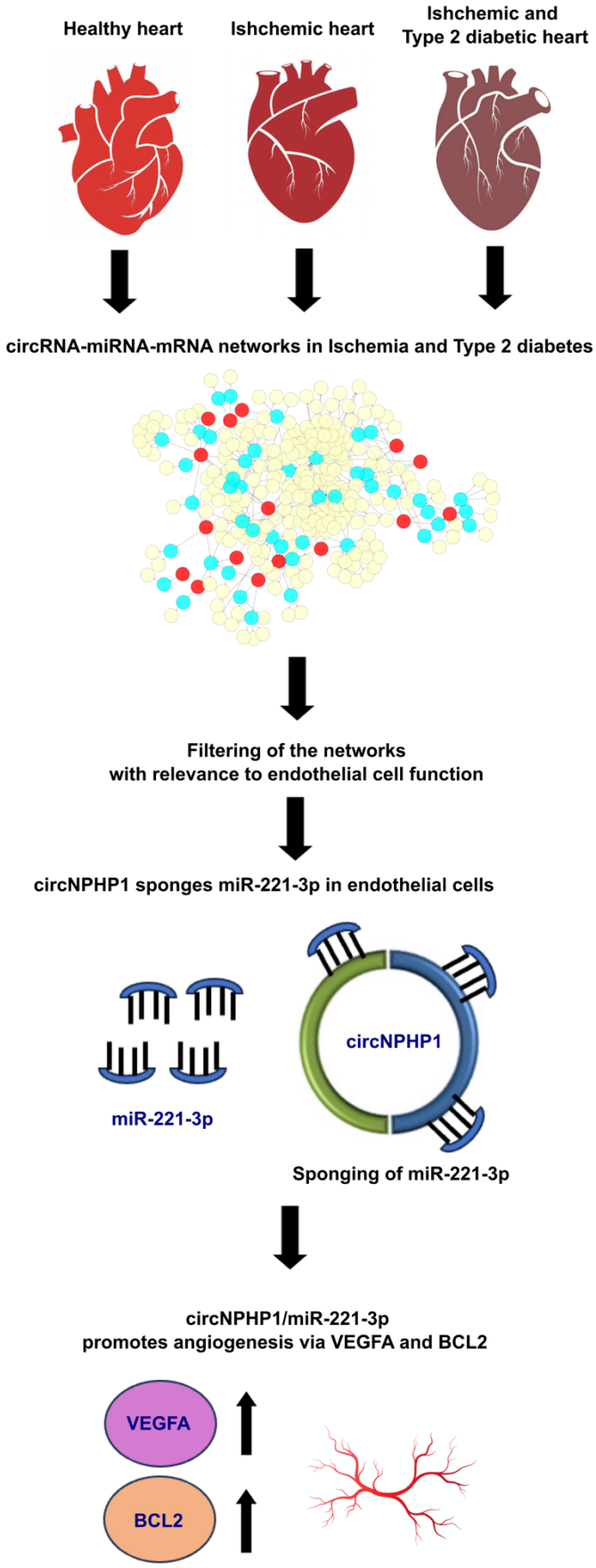
Healthy heart
Ishchemic heart
Ishchemic and
Type 2 diabetic heart
circRNA-miRNA-mRNA networks in Ischemia and Type 2 diabetes
Filtering of the networks
with relevance to endothelial cell function
circNPHP1 sponges miR-221-3p in endothelial cells
miR-221-3p
circNPHP1
Sponging of miR-221-3p
circNPHP1/miR-221-3p
promotes angiogenesis via VEGFA and BCL2
VEGFA
BCL2

Novelty and Significance
What Is Known?

- CircRNAs are covalently bonded loop structures that sponge miRNAs and regulate their target genes.
- CircRNAs have previously been associated to cardiovascular disease but not in the setting of ischemic heart disease and Type 2 diabetes.
- Linear NPHP1 has been implicated in kidney disease.

What New Information Does This Article Contribute?

- We found a novel CircRNA-miRNA-mRNA networks in IHD and Type 2 diabetes.
- CircNPHP1 regulates angiogenesis and proliferation in the cardiac ECs exposed to conditions mimicking IHD and Type 2 diabetes.
- We elucidated a novel pro-angiogenic subnetwork commanded by circNPHP1/miR-221-3p/BCL2/VEGFA.

IHD is a major cause of mortality every year. This is the first time that circRNAs and their networks have been mapped in IHD and Type 2 diabetes using clinical samples from left ventricle biopsies of cardiac surgery patients and a streamlined bioinformatics pipeline. We identified a sub-network involving circNPHP1, its sponged miRNAs and downstream target mRNAs. From this we elucidated a novel pro-angiogenic arc (circNPHP1/miR-221-3p/BCL2/VEGFA) that regulates angiogenesis and proliferation in cardiac endothelial cells exposed to conditions mimicking IHD and Type 2 diabetes.

Figure 1

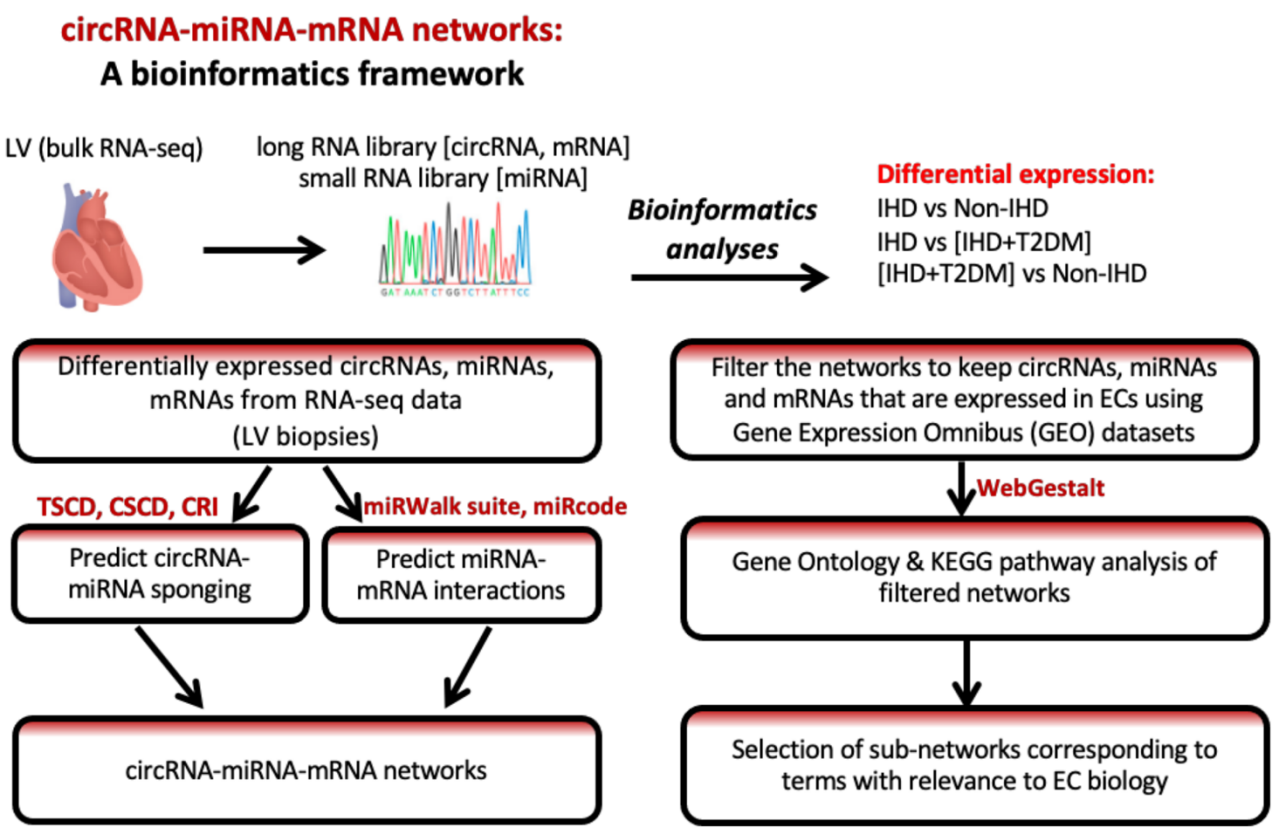

Figure 1: A bioinformatics framework to build circRNA-miRNA-mRNA networks After extracting RNAs (circRNAs, miRNAs and mRNAs) from RNA sequencing data on LV biopsies of cardiac surgery patients [IHD(N=12), IHD+T2DM(N=11), non-IHD(N=12)], differential expression analyses were performed. Next, circRNA-miRNA sponging interactions were predicted using three databases: TSCD, CSCD and CRI. miRNA-mRNA interactions were predicted using miRWalk suite and miRcode. Furthermore, only those interactions were kept where the connecting nodes (circRNAs, miRNA and mRNAs) were expressed in the ECs (using published EC datasets from GEO). Gene Ontology and KEGG pathway analyses were subsequently performed on these filtered networks. Sections of the network that mapped to processes corresponding to EC biology were further analysed.

Figure 2

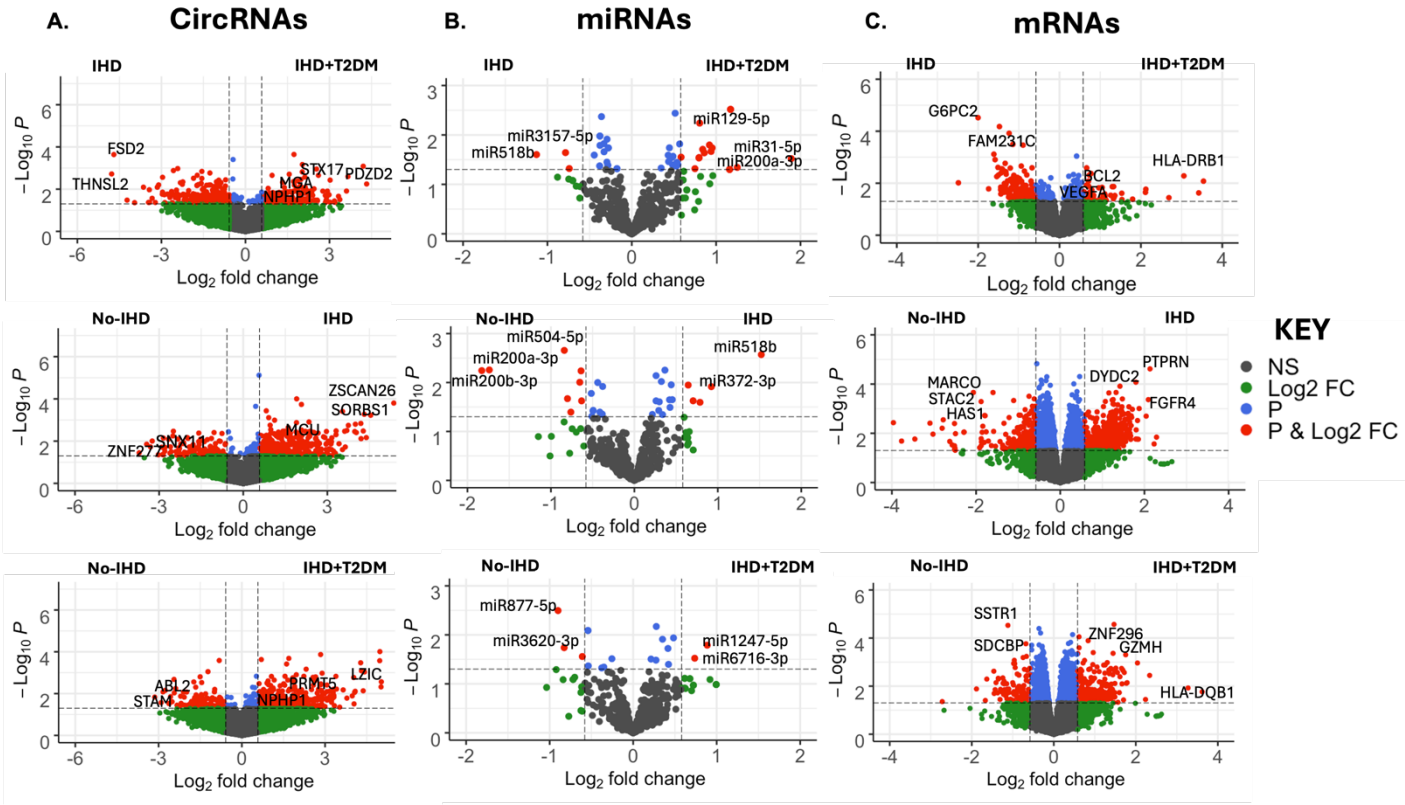

Figure 2: Differential expression analyses

(A-C) CircRNAs, miRNAs and mRNAs were identified following the pipeline outlined in methods [IHD(N=12), IHD+T2DM(N=11), non-IHD(N=12)]. Differential expression analyses were performed on normalised and log-transformed counts using the R package *Limma.* Three comparisons were performed (IHD+T2DM vs IHD), (IHD vs non-IHD) and (IHD+T2DM vs non-IHD). The corresponding differentially expressed circRNAs, miRNAs and mRNAs were plotted in a volcano plot with log2 fold change (FC) on the x-axis and -log10 Pvalues on the y axis. CircRNAs, miRNAs and mRNAs that passed the log2 FC threshold of +/-0.58 and Pvalue <= 0.05 are shown in red, those that just pass the FC threshold are in green and those that only pass the Pvalue threshold are in blue.

A. **IHD network (enriched in ECs) and corresponding GO biological processes and KEGG pathways**

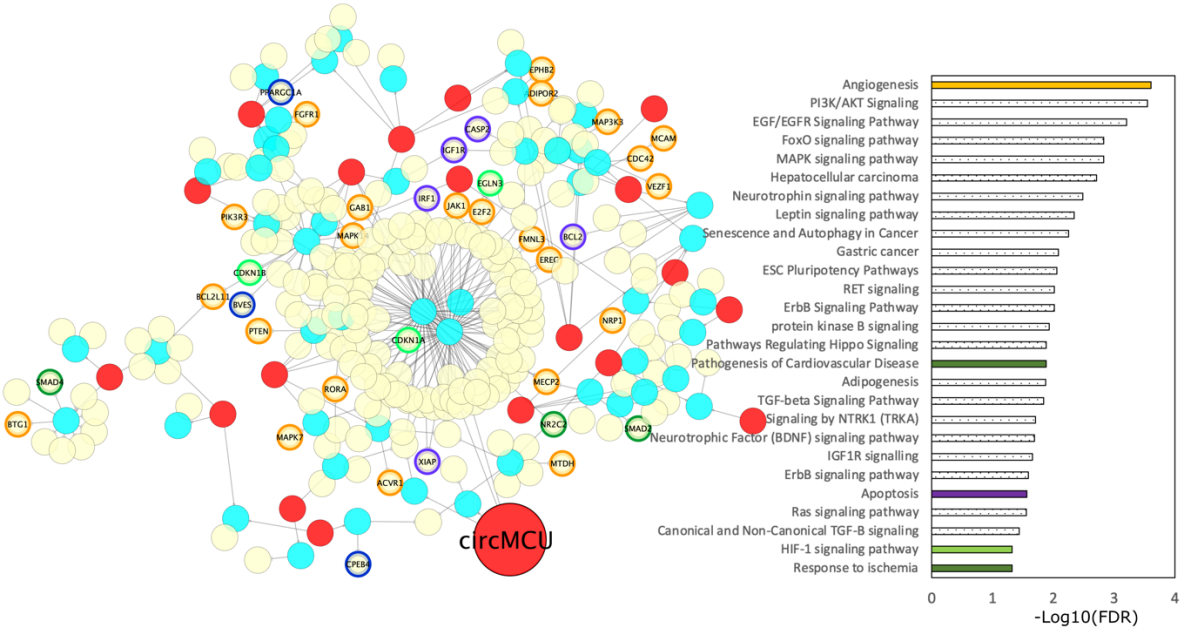

B. **IHD+T2DM network (enriched in ECs) and corresponding GO biological processes and KEGG pathways**

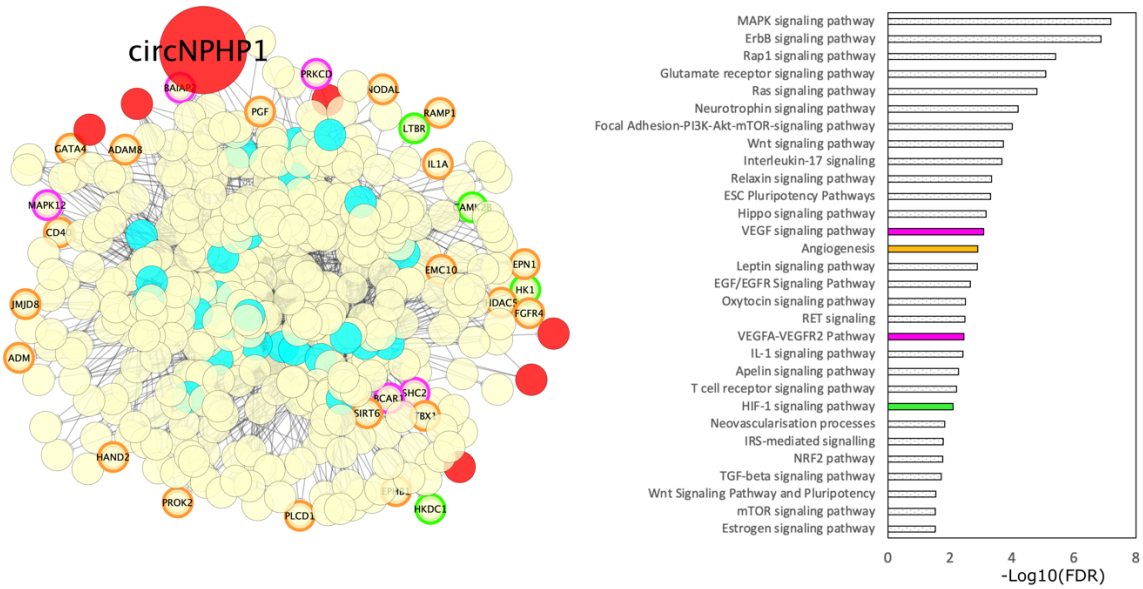

C. **T2DM network (enriched in ECs) and corresponding GO biological processes and KEGG pathways**

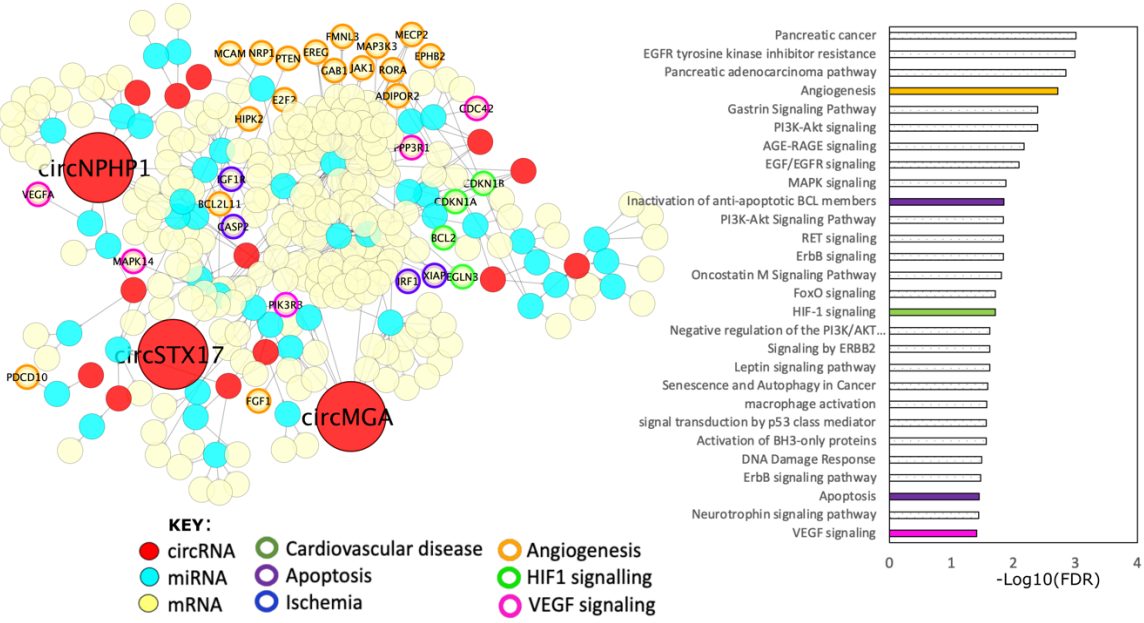

Figure 3: Predicted circRNA-miRNA-mRNA networks in the heart ECs

(A-C) circRNA-miRNA-mRNA networks were constructed in Cytoscape using predicted interactions between circRNAs, miRNAs and mRNAs in IHD (+/- T2DM) (using in-house LV biopsies and heart ECs [GEO data]). All nodes (circRNAs, miRNA and mRNAs) shown in the network are expressed in LV biopsies and ECs. The networks show circRNAs in red, miRNAs in cyan and mRNAs in yellow. The top significantly upregulated circRNAs are enlarged and labelled. Following Gene Ontology (GO) and KEGG pathway analyses, all significant GO biological processes and KEGG pathways (passing threshold of FDR <= 0.05) were plotted as a bar graph with -log10(FDR) on the x-axis. Moreover, pathways relevant to EC biology are highlighted in the graph as solid colors. The corresponding genes (downstream targets of circRNAs and miRNAs) are outlined with the color of the relevant pathways. Genes that correspond to more than 1 pathway are outlined with multiple colors.

(A) Network constructed from IHD vs non-IHD comparison: The top circRNAs circMCU. Of note are pathways related to cardiovascular disease, apoptosis, ischemia, angiogenesis and HIF1 signalling.

(B) Network constructed from IHD+T2DM vs non-IHD comparison: The top circRNAs include circNPHP1. Of note are pathways related to VEGF signalling, angiogenesis and HIF1 signalling.

(C) Network constructed from IHD+T2DM vs IHD comparison: The top circRNAs include circNPHP1, circSTX17 and circMGA. Of note are pathways related to VEGF signalling, apoptosis, angiogenesis and HIF1 signalling.

Figure 4

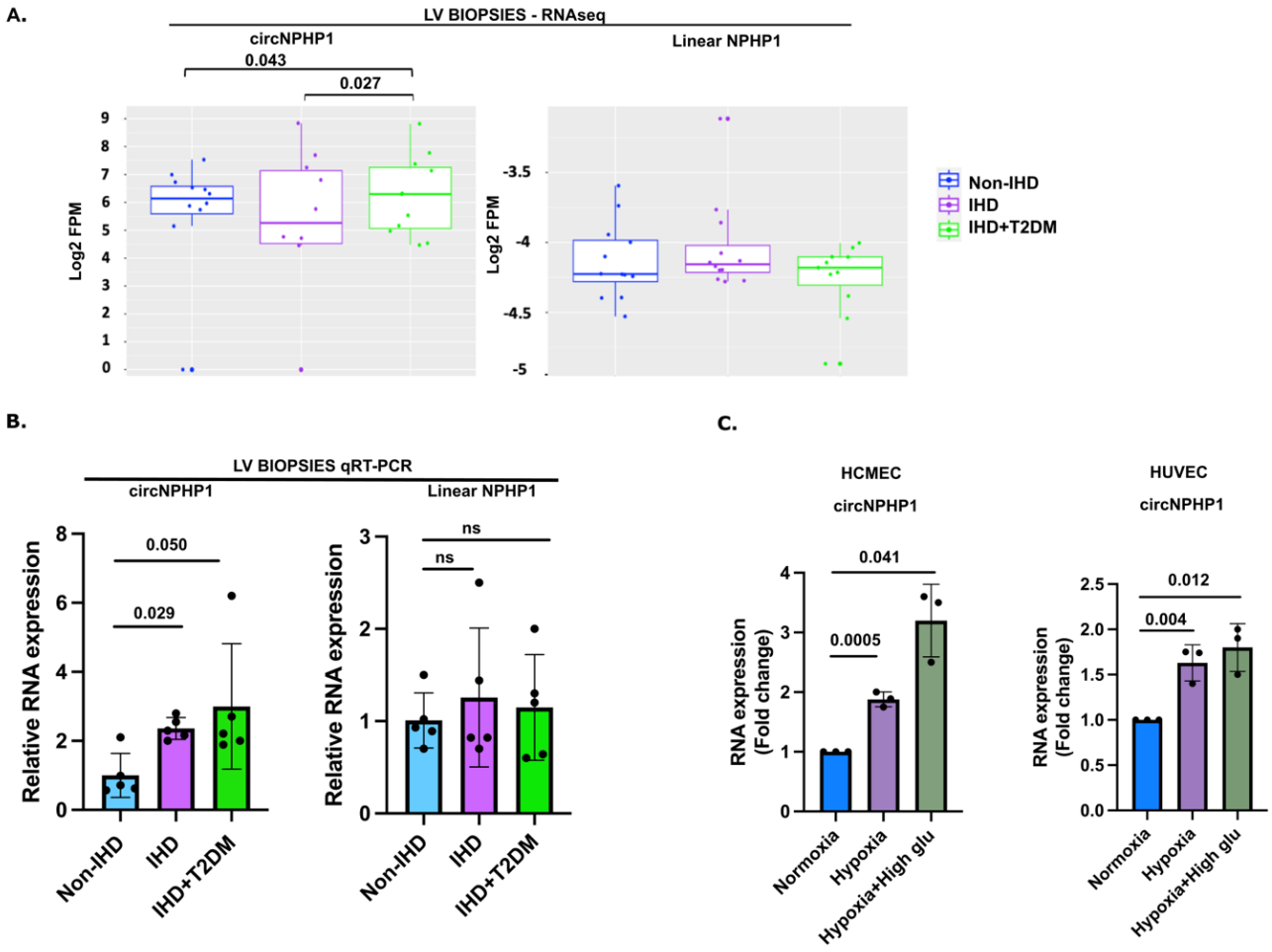

Figure 4. CircNPHP1 is upregulated in IHD and diabetic conditions in the LV biopsies and ECs

(A) RNAseq: Log-transformed normalised (FPM) values of circNPHP1 and linear NPHP1 are plotted as boxplot. CircNPHP1 is significantly upregulated in IHD+T2DM as compared to IHD and non-IHD (Pvalue<=0.05). Linear NPHP1 is expressed at very low levels and does not change between the different patient groups [IHD(N=12), IHD+T2DM(N=11), non-IHD(N=12)].

(B) Quantitative real-time polymerase chain reaction (qRT-PCR) analysis of circNPHP1 (left panel) and linear NPHP1 (right panel) of LV biopsies from non-IHD (N=5), IHD (N=5), IHD+T2DM (N=5). 18S is used as housekeeping gene. Results were assessed by Kruskal-Wallis test followed by Dunn's multiple comparison to non-IHD group. P values are indicated accordingly, P>0.05 is indicated as ns [nonsignificant].

(C) Human cardiac microvascular endothelial cells (HCMEC) (left panel) and human umbilical vein endothelial cells (HUVEC) (right panel) were cultured in normal conditions, hypoxia (1% Oxygen) and hypoxia-high glucose (25Mm glucose) conditions respectively. After 48 hours, cells were harvested for qRT-PCR for the analysis of circNPHP1 (N=3). Fold change in RNA expression is relative to normoxia; 18S is used as housekeeping gene. Results were assessed by 1-way ANOVA (Dunnett's post hoc test). P values are indicated accordingly, P>0.05 is indicated as ns [nonsignificant].

Figure 5

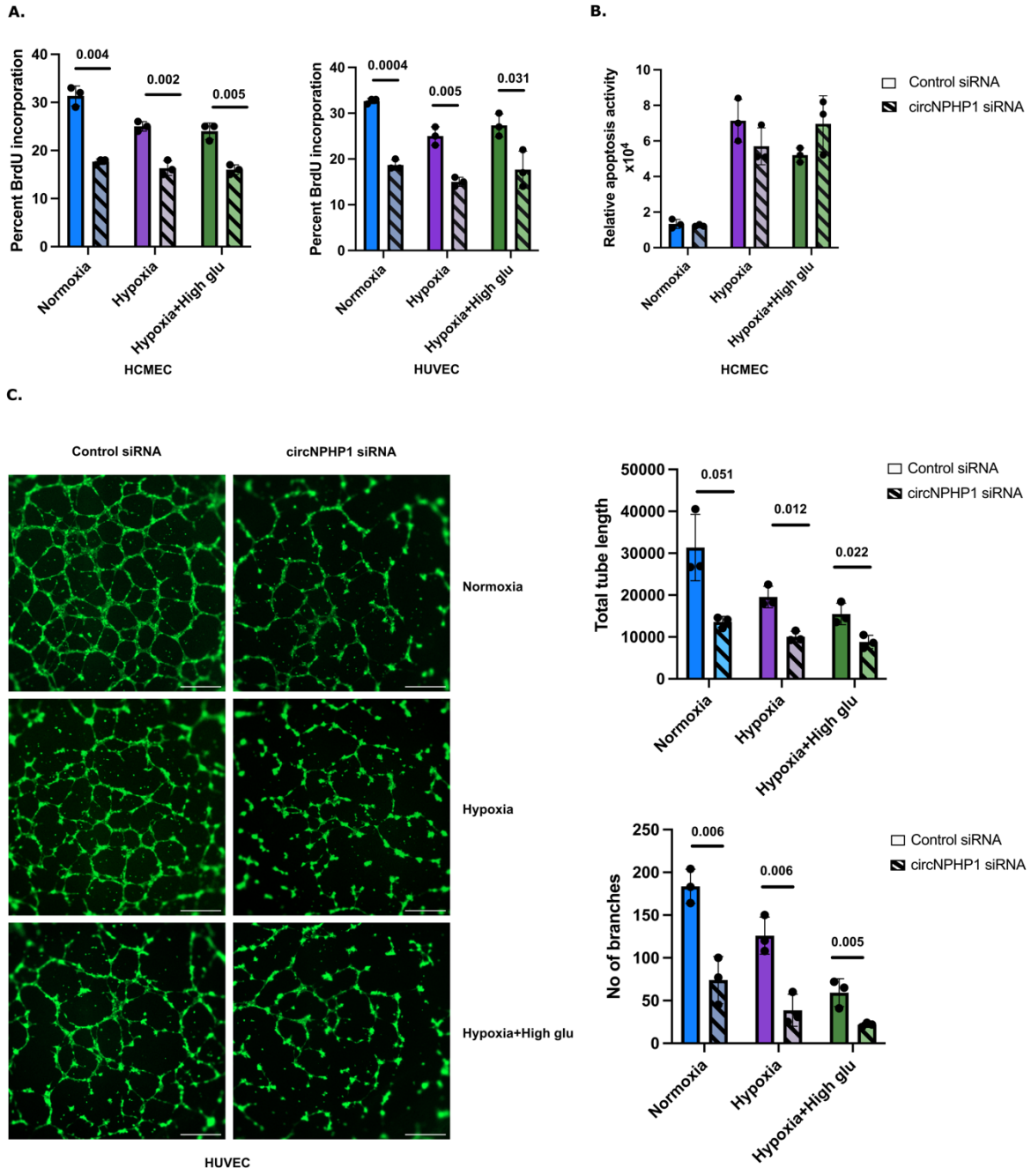

Figure 5. CircNPHP1 is involved in proliferation and angiogenesis in the ECs

(A) HCMECs (left panel) and HUVECs (right panel) were transfected with 30nM of circNPHP1 siRNA or control siRNA, and cultured in normal conditions, hypoxia (1% Oxygen) and hypoxia-high glucose (25mM glucose) conditions respectively. 48 hours

post transfection, cells were harvested for proliferation assay (BrDU incorporation) (N=3), and (B) HCMEC: apoptosis assay (Annexin V assay) (N=3).

(C) HUVECs were transfected with 30nM of circNPHP1 siRNA or control siRNA, and cultured in normal conditions, hypoxia (1% Oxygen) and hypoxia-high glucose (25mM glucose) conditions respectively. 48 hours post transfection, cells were seeded on a 96-well plate containing Growth Factor Reduced Matrigel and cultured in similar conditions for 8 hours to determine cord formation. Representative images of angiogenesis (stained with Phalloidin, scale bar: 500 μM) (left panel). Histograms depicting the total tube length and number of branches quantified from the angiogenesis assay (right panel) (N=3).

Results in **(**A–C) were by unpaired Student *t* test between control siRNA and circNPHP1siRNA among the three groups respectively. P values are indicated accordingly, P>0.05 is indicated as ns [nonsignificant].

Figure 6

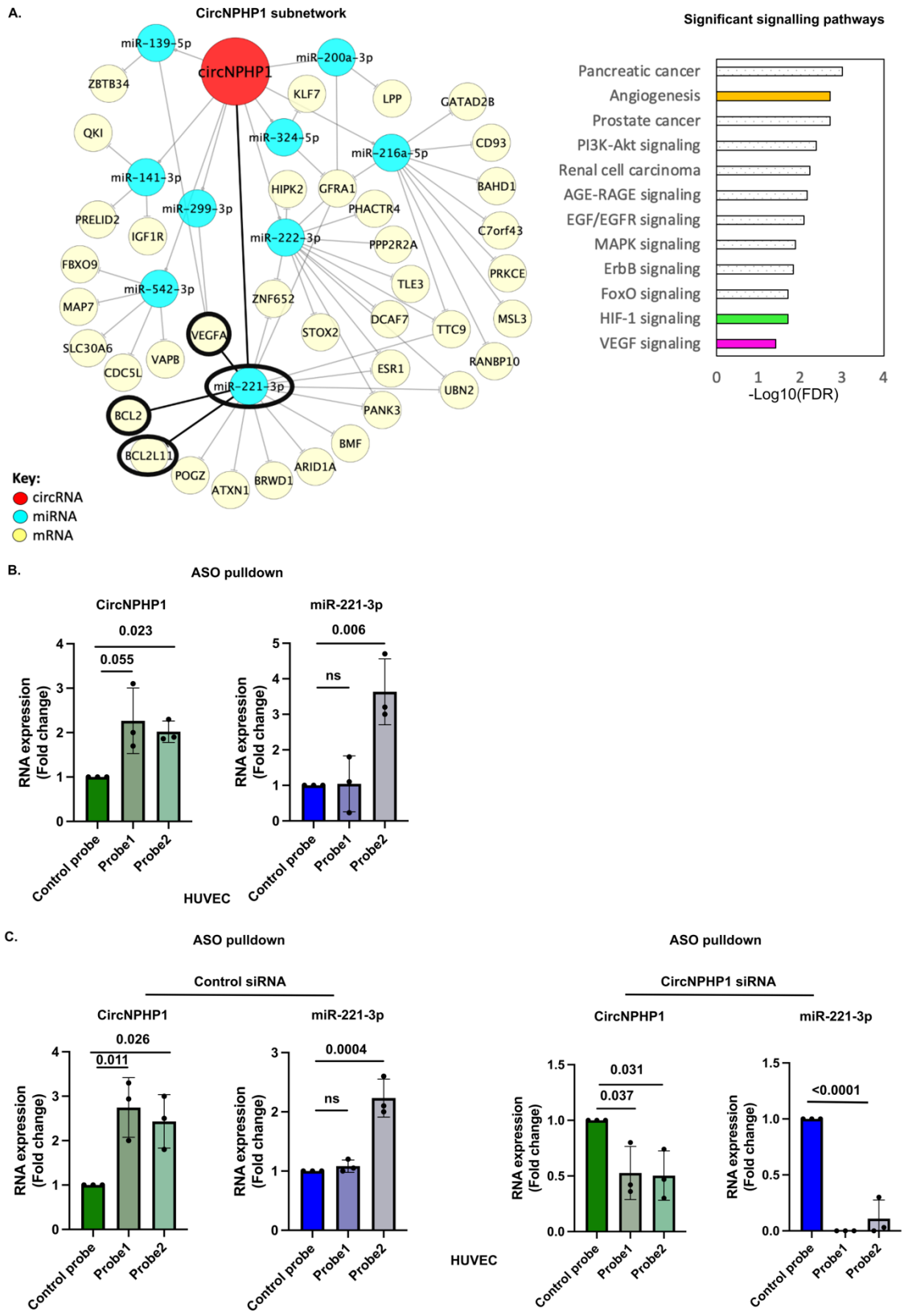
A.
CircNPHP1 subnetwork
circNPHP1
miR-139-5p
miR-200a-3p
miR-324-5p
miR-216a-5p
miR-141-3p
miR-299-3p
miR-222-3p
miR-542-3p
miR-221-3p
ZBTB34
QKI
KLF7
LPP
GATAD2B
CD93
BAHD1
HIPK2
GFRA1
PHACTR4
PRELID2
IGF1R
PPP2R2A
C7orf43
FBXO9
PRKCE
TLE3
MAP7
ZNF652
DCAF7
TTC9
MSL3
VEGFA
STOX2
SLC30A6
VAPB
RANBP10
CDC5L
ESR1
UBN2
BCL2
PANK3
BMF
BCL2L11
ARID1A
POGZ
BRWD1
ATXN1
Key:
circRNA
miRNA
mRNA
Significant signalling pathways
Pancreatic cancer
Angiogenesis
Prostate cancer
PI3K-Akt signaling
Renal cell carcinoma
AGE-RAGE signaling
EGF/EGFR signaling
MAPK signaling
ErbB signaling
FoxO signaling
HIF-1 signaling
VEGF signaling
0 1 2 3 4
-Log10(FDR)
B.
ASO pulldown
CircNPHP1
0.023
0.055
RNA expression (Fold change)
Control probe
Probe1
Probe2
miR-221-3p
0.006
ns
HUVEC
C.
ASO pulldown
Control siRNA
CircNPHP1
0.026
0.011
miR-221-3p
0.0004
ns
ASO pulldown
CircNPHP1 siRNA
CircNPHP1
0.031
0.037
miR-221-3p
<0.0001
HUVEC

Figure 6. CircNPHP1 binds miR-221-3p and constitutes a pro-angiogenic sub-network.

(A) CircNPHP1 was found to be enriched in IHD+T2DM as well as T2DM. We therefore extracted the miRNAs and mRNAs that were connected to circNPHP1 to analyse the interactions in greater detail. Pathway analyses on this subnetwork of circNPHP1 revealed VEGF signalling and angiogenesis as significantly enriched. The arc consisting of circNPHP1, its sponged miRNA partner (miR-221-3p) and downstream targets that were validated (VEGFA, BCL2, BCL2L11) are bold in black.

(B) HUVEC cell extracts were incubated with biotinylated ASO control probe, probe 1 and probe 2 respectively (see details in methods) for pulldown of circNPHP1 using streptavidin beads. Subsequently, RNA was isolated and subjected to qRT-PCR for the analysis of circNPHP1 (left panel) and miR-221-3p (right panel). Fold enrichment was calculated in the pulldown samples with probe 1 and probe 2 against the control probe pulldown. 18S and U6 were used as reference genes to normalize for circNPHP1 and miR-221-3p respectively (N=3).

(C) HUVECs were transfected with 30nM of circNPHP1 short interfering RNA (siRNA) or control siRNA. 48 hours post transfection, cells were harvested and incubated with biotinylated ASO control probe, probe 1 and probe 2 respectively for pulldown of circNPHP1 using streptavidin beads. Subsequently, RNA was isolated and subjected to qRT-PCR for the analysis of circNPHP1, linear NPHP1 and miR-221-3p. Fold enrichment was calculated in the pulldown samples with probe 1 and probe 2 against the control probe pulldown. 18S and U6 were used as reference genes to normalize for circNPHP1, linear NPHP1 and miR-221-3p respectively (N=3).

Results were assessed by 1-way ANOVA (Dunnett's post hoc test). P values are indicated accordingly, $P>0.05$ is indicated as ns [nonsignificant].

Figure 7

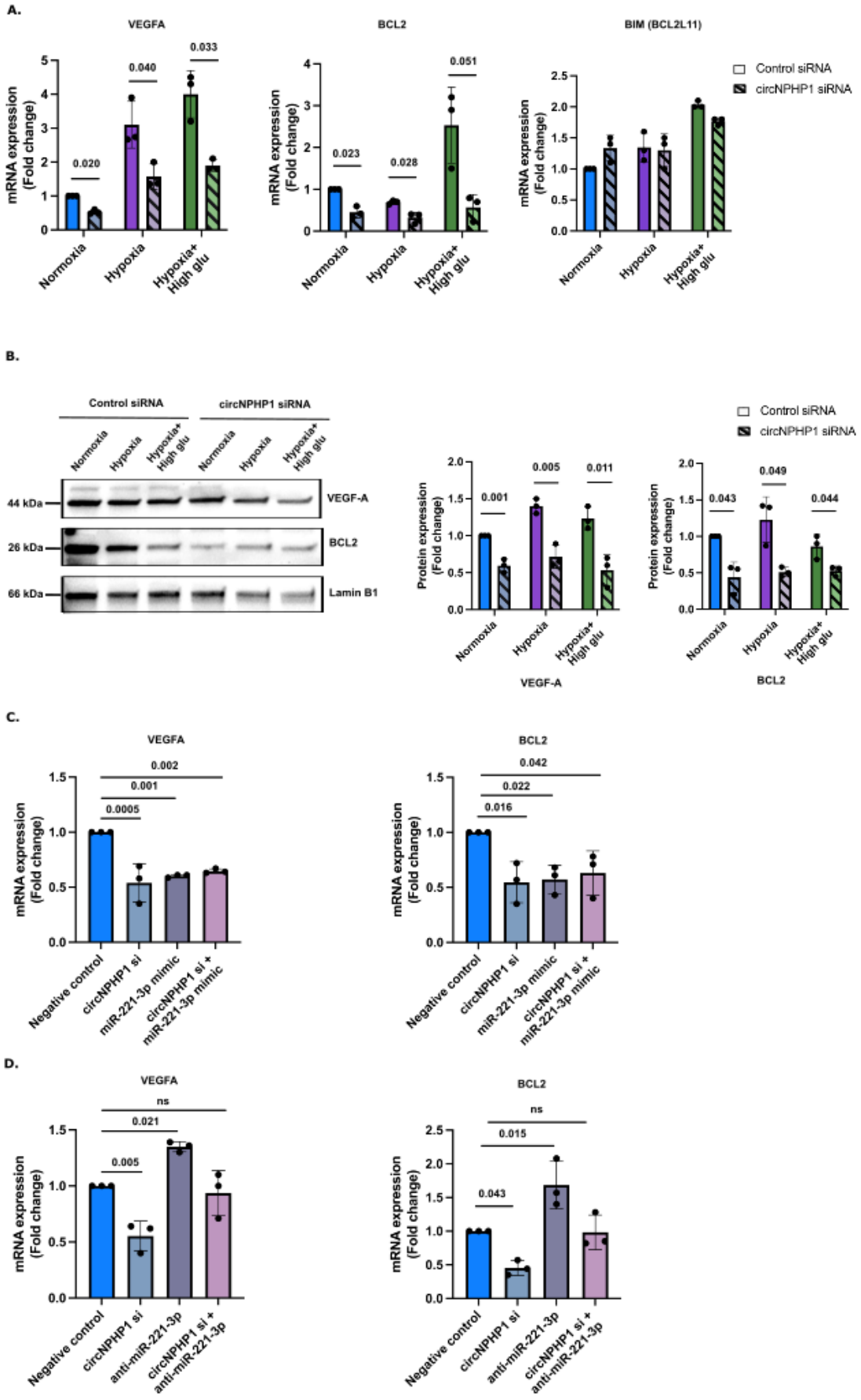
A.
VEGFA
BCL2
BIM (BCL2L11)
mRNA expression (Fold change)
0.020
0.040
0.033
0.023
0.028
0.051
Control siRNA
circNPHP1 siRNA
Normoxia
Hypoxia
Hypoxia+ High glu
B.
Control siRNA
circNPHP1 siRNA
44 kDa
26 kDa
66 kDa
VEGF-A
BCL2
Lamin B1
Protein expression (Fold change)
0.001
0.005
0.011
0.043
0.049
0.044
C.
0.002
0.001
0.0005
0.042
0.022
0.016
Negative control
circNPHP1 si
miR-221-3p mimic
circNPHP1 si + miR-221-3p mimic
D.
ns
0.021
0.005
0.015
0.043
anti-miR-221-3p
circNPHP1 si + anti-miR-221-3p

Figure 7. CircNPHP1 sponges miR-221-3p and regulates its target genes

(A) HUVECs were transfected with 30nM of circNPHP1 siRNA or control siRNA, and cultured in normal conditions, hypoxia (1% Oxygen) and hypoxia-high glucose (25mM glucose) conditions respectively. 48 hours post transfection, cells were harvested for qRT-PCR for the analysis of VEGFA, BCL2 and BIM (N=3). Fold change in mRNA expression is relative to normoxia; 18S is used as housekeeping gene.

(B) HUVECs were transfected with 30nM of circNPHP1 siRNA or control siRNA, and cultured in normal conditions, hypoxia (1% Oxygen) and hypoxia-high glucose (25mM glucose) conditions respectively. 48 hours post transfection, cells were harvested for western blot analysis of VEGF-A and BCL2 (N=3). Images shown are representative (left panel). Histograms showing western blot quantification is expressed as fold change against normoxia and normalized to Lamin B1 (loading control) (right panel).

(C) HUVECs were transfected with 30nM of circNPHP1 siRNA, miR-221-3p mimic respectively or in combination. Combination of control siRNA and control mimic is used as negative control. 48 hours post transfection, cells were harvested for qRT-PCR for the analysis of VEGFA and BCL2 (N=3).

(D) HUVECs were transfected with 30nM of circNPHP1 siRNA, anti-miR-221-3p respectively or in combination. Combination of control siRNA and anti-miRNA control is used as negative control. 48 hours post transfection, cells were harvested for qRT-PCR for the analysis of VEGFA and BCL2 (N=3).

In (C-D) fold change in mRNA expression is relative to negative control; 18S is used as housekeeping gene.

Results in **(**A–B) were assessed by unpaired Student *t* test between control siRNA and circNPHP1siRNA among the three groups respectively and in (C-D) by 1-way ANOVA (Dunnett's post hoc test). P values are indicated accordingly, P>0.05 is indicated as ns [nonsignificant].